Molecular dynamics simulations of disjoining pressure effect in ultra-thin water film on a metal surface

H. Hu and Y. Sun[a)]
Department of Mechanical Engineering and Mechanics, Drexel University, Philadelphia, Pennsylvania 19104, USA

(Received 10 October 2013; accepted 10 December 2013; published online 30 December 2013)

Molecular dynamics (MD) simulations are used to examine the disjoining pressure effect of a water thin film adsorbed on a metal surface. The model was validated against experiments and verified against previous MD simulations. The variation of vapor pressure with film thickness was examined for a water thin film adsorbed on a gold surface. The results agree well with the classic disjoining pressure theory without surface charges and show that liquid layering does not affect disjoining pressure. However, surface charges of the gold substrate enhance the disjoining pressure of the water thin film, consistent with experimental evidences for polar liquids. © *2013 AIP Publishing LLC*.
[http://dx.doi.org/10.1063/1.4858469]

Nanoscale thin liquid films are important in lubrication,[1] wetting and spreading,[2–4] thin film evaporation,[5–11] and boiling heat transfer.[12,13] The thin films are intermediate liquid phases between two surfaces, which can be any combination of solid, liquid, or vapor, with nanometer separation. It is well known that the pressure in a thin liquid film is different from that in the bulk liquid; this pressure difference is called the disjoining pressure.[14] Hamaker[15] developed the original model to predict the disjoining pressure, P_D, as a function of the film thickness δ as follows:

$$P_D = -\frac{A}{6\pi\delta^3}, \tag{1}$$

where A is the Hamaker constant, derived based on pairwise interatomic interactions neglecting the role of any intervening media between the two surfaces of the thin film. Lifshitz[16] and Ninham[17] further extended the theory to account for many-body interatomic interactions and the effect of intervening media by introducing the dielectric constant and refractive index of the thin film into the expression for the Hamaker constant. The resulting Hamaker constant based on the Lifshitz theory showed good agreement with experimental results for the interactions between two solid surfaces (e.g., mica, gold, sapphire) across a water film.[18–21] Herein, the term "classic disjoining pressure theory" refers to Eq. (1).

For a thin monatomic liquid film between a solid wall and a vapor, the vapor pressure[22,23] predicted using the classic disjoining pressure theory and the ideal gas assumption matches well with experiments.[24] Panella *et al.*[25] measured the equilibrium thicknesses of adsorbed liquid films on metal surfaces under various vapor pressures and showed that while the classic theory accurately predicts the film thickness for simple nonpolar liquids (e.g., Ne) where van der Waals forces dominate, it underestimates the film thickness for polar liquids (e.g., water) as reported earlier by Derjaguin and Churaev.[26] In addition, for polar liquids, besides the need to account for electrostatic interactions, a more accurate equation of state (EOS) rather than the ideal gas law is needed to relate the vapor pressure with its density.

Molecular dynamic (MD) simulations have become a powerful tool to examine properties of nanoscale thin films. A number of MD studies have been reported to investigate the disjoining pressure effects in thin films of nonpolar liquids.[23,27–32] Bhatt *et al.*[27] and Han[33] found that disjoining pressures calculated by MD simulations for free standing and adsorbed liquid films were much larger than those predicted by the classic theory. In contrast, MD simulations performed by Carey and Wemhoff[23] and Yu and Wang[30] predicted the disjoining pressure in good agreement with the classic theory. However, no direct comparison with experiments has been reported in previous MD studies that are to date only limited to nonpolar liquids using the Lennard-Jones potential.

In this letter, MD simulations are performed to examine the validity of the classic disjoining pressure theory in a water thin film between a solid wall and water vapor. The model is first validated against experiments[20] and verified using previous MD results for a nonpolar liquid.[23] The vapor pressure of a water thin film of different thicknesses adsorbed on a gold surface is then calculated, and the results are compared with the classic theory using the equation of state based on a six-order virial expansion. Finally, the role of electrostatic interactions between gold surface and water film on the disjoining pressure is explored.

In order to calculate the interaction energy between two gold surfaces across a water film to validate against Derjaguin's experiments,[20] four simulation systems, namely, Au-H_2O(l)-Au, Au-H_2O(l)-H_2O(v)-Au, Au-vacuum-Au, and H_2O(v)-H_2O(l)-H_2O(v), with the same surface area (S) are used as shown in Fig. 1. Each substrate consists of a $12 \times 12 \times 12$ FCC gold lattice with the lattice constant of 4.08Å. The water film thickness varies from 0.6 nm to 1.8 nm. For the Au-H_2O(l)-H_2O(v)-Au system, a 4 nm water vapor was in between water film and gold substrate and two gold surfaces were separated by 4 nm vacuum for the Au-vacuum-Au system. The H_2O(v)-H_2O(l)-H_2O(v) system

a)Author to whom correspondence should be addressed. Electronic mail: ysun@coe.drexel.edu. Tel.: +1(215)895-1373. Fax: +1(215)895-1478.

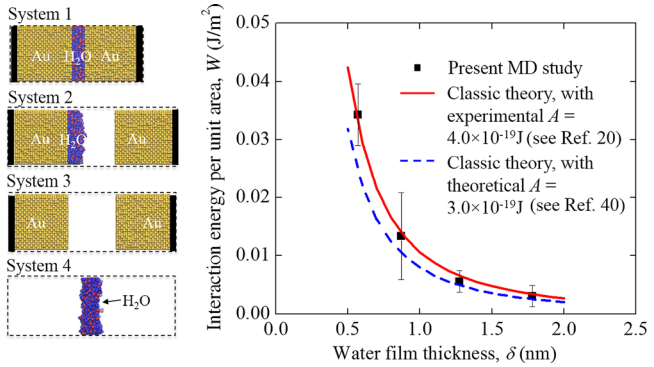

FIG. 1. Comparison of the MD calculated and theory predicted interaction energy per unit area between gold surfaces across a water thin film at 300 K. The lines depicting the classic disjoining pressure theory are based on Eq. (2) with Hamaker constants from experiments (see Ref. 20) and theoretical calculations (see Ref. 40), respectively.

consists of a water thin film equilibrated with its own vapor. The embedded-atom method (EAM)[34] was applied for interactions between gold atoms. The TIP4P-Ew water model[35] was used for water-water interactions, where particle-particle particle-mesh (PPPM) was used to account for long-range Coulombic interactions and the SHAKE algorithm[36] was applied to keep the water molecules rigid. A 12-6 Lennard-Jones potential with a cutoff of 9 Å was used to describe the water-gold interactions, where the parameters were $\varepsilon_{Au/O} = 8.3\,\text{kJ/mol}$, $\sigma_{Au/O} = 2.95\,\text{Å}$, $\varepsilon_{Au/H} = 0$, and $\sigma_{Au/H} = 0$.[37] All simulations were performed using LAMMPS.[38] Each system was equilibrated in an NVT (N the number of atoms, V the volume, and T the temperature) ensemble at 300 K for 1 ns where the total energy of the system was averaged from 500 ps to 1 ns. The interaction energy per unit area, W, between two gold surfaces across a thin water film was calculated with details shown in the supplemental material.[39]

Figure 1 shows the comparison of the MD calculated and classic theory predicted interaction energy per unit area between two gold surfaces across a thin water film as a function of the film thickness at 300 K. The error bars are obtained by using five different random velocity seeds for temperature initializations. The classic disjoining pressure theory gives the following expression for the interaction energy per unit area:[22]

$$W = -\frac{A}{12\pi\delta^2}. \tag{2}$$

Two values for the Hamaker constant are used: the theoretical prediction of 3×10^{-19}J based on the Lifshitz theory[40] and the experimental measurement of 4×10^{-19}J.[20] As shown in Fig. 1, the MD simulated interaction energy lies in between two theoretical predictions for all tested film thicknesses, indicating that our MD model correctly accounts for gold-gold interactions across a water thin film.

The MD model is then verified against Carey and Wemhoff[23] for an argon thin film adsorbed on a solid wall using the same force fields and properties but a slightly different setup. Figure 2 shows the comparison of the present results with those of Carey and Wemhoff[23] for the vapor pressure near an argon thin film adsorbed on a L-J solid with

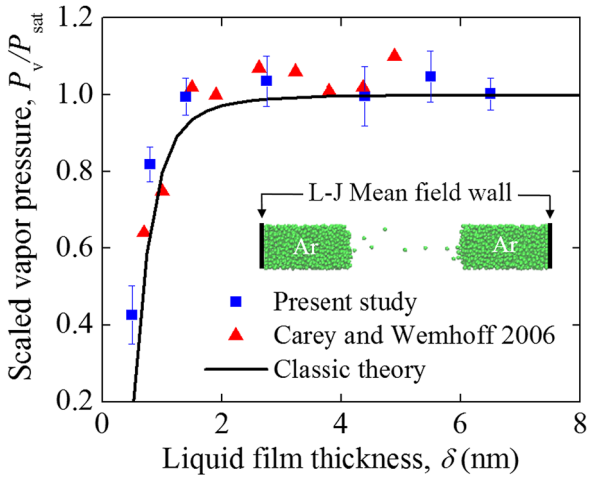

FIG. 2. Comparison of the present MD simulation and that of Carey and Wemhoff (see Ref. 23) for the vapor pressure near an argon thin film with different film thicknesses at 90 K. The classic disjoining pressure theory curve is calculated using Eq. (3).

varying film thickness at 90 K. Here, the vapor pressure is calculated using the classic disjoining pressure theory[23] via

$$\frac{P_v}{P_{sat}} = \exp\left\{-\frac{A}{6\pi\rho_f k_B T}\frac{1}{\delta^3}\right\}, \tag{3}$$

where P_v is the vapor pressure near the thin film, P_{sat} the saturation pressure at temperature T, ρ_f the density of bulk liquid, and k_B the Boltzmann constant. Three differences between the present simulation setup and that of Carey and Wemhoff[23] are worth noting: (i) two liquid films 10 nm apart were equilibrated in a NVT ensemble instead of using one liquid film with flux boundary and equilibrated in a μPT ensemble (μ is the chemical potential, P the pressure, and T the temperature); (ii) the argon vapor pressure was directly calculated by summing up the local pressure tensor[41] instead of using the kinetic theory; and (iii) a broader range of liquid film thickness was examined. Despite these differences, the vapor pressure calculated in the present MD simulation agrees well with that of Carey and Wemhoff,[23] along with the theory prediction based on Eq. (3) as shown in Fig. 2, indicating that the simulation setup used here (inset of Fig. 2) is adequate for predicting the disjoining pressure effect in thin films.

MD simulations are then performed for a water thin film adsorbed on a gold surface. As shown in the inset of Fig. 3(b), two water films are separated 10 nm apart and both a mean field potential and a real gold lattice are used to represent the solid wall for the effect of crystalline structure on disjoining pressure. For the case of a mean field wall, a 9-3 Lennard-Jones mean field potential is applied at both ends of the system in z, periodic boundaries are in x and y, and other parameters are $A = 7.09 \times 10^{-19}$J, $\rho_f = 1.47 \times 10^{28}\text{m}^{-3}$, and $D_m = 2.95$Å. For the system with a real gold wall, periodic boundary conditions are applied in all directions and two $12 \times 12 \times 12$ FCC gold lattices are used at both ends in z, where two atomic layers are frozen at each end. Two potentials are used for the water-gold interactions, respectively: (i) the 12-6 Lennard-Jones potential and (ii) the modified Spohr potential accounting for both Au-O and Au-H

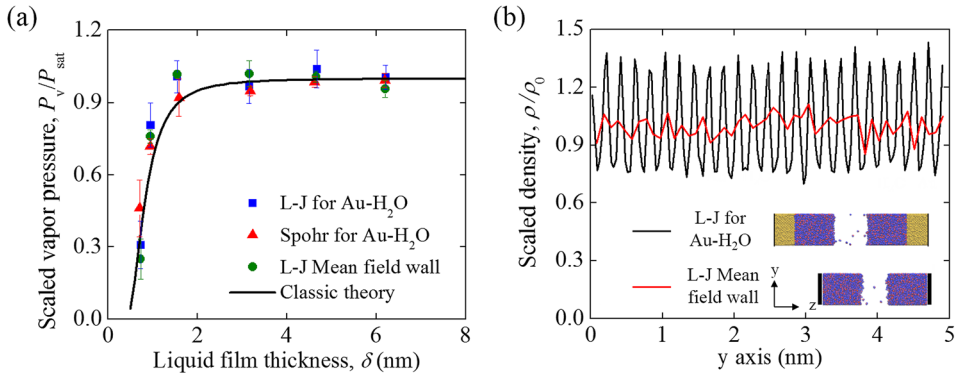

FIG. 3. (a) Comparison of the present MD simulation and the classic theory for the vapor pressure near a water thin film adsorbed on a gold surface with different film thicknesses at 400 K. The classic disjoining pressure theory curve is calculated based on Eq. (6). (b) Comparison of the scaled density profile of water film along y on a mean filed wall against a gold lattice. The inset shows the schematic of thin water films on gold surfaces.

interactions with parameters taken from Dou *et al.*[42] The system is equilibrated using NVT at 400 K for 1 ns. The total vapor pressure is calculated by summing up the local pressure tensor[41] in the vapor region and averaged from 500 ps to 1 ns.

When a vapor and a thin liquid film are in equilibrium, the chemical potentials, μ, of the vapor and liquid have to be equal, which yields

$$\int v_v dP_v = v_l(P_l - P_{sat}) + N_A\Phi_{wall}, \tag{4}$$

where N_A is the Avogadro constant and Φ_{wall} is the wall potential. Here, the 6th-order virial expansion is used for the EOS of water vapor

$$\frac{Pv}{RT} = 1 + \sum_{n=2}^{6}\frac{B_n(T)}{v^{n-1}}, \tag{5}$$

where the virial coefficients $B_2 = -0.67032\text{L/mol}$, $B_3 = -0.42599(\text{L/mol})^2$, $B_4 = -0.3291(\text{L/mol})^3$, $B_5 = 2.2135(\text{L/mol})^4$, and $B_6 = -1.07155(\text{L/mol})^5$ at 400 K (Ref. 43) are used to account for two-body and many-body interactions. The Φ_{wall} term uses the 9-3 Lennard-Jones mean field potential for water-gold interactions. Equation (5) hence becomes the following expression of vapor pressure near a water thin film:

$$\frac{P_v}{P_{sat}} = x\frac{v_{sat}^5 + \sum_{n=2}^{6} v_{sat}^{6-n}B_n x^{n-1}}{v_{sat}^5 + \sum_{n=2}^{6} v_{sat}^{6-n}B_n}, \tag{6}$$

where $x = v_{sat}/v_v$ can be calculated by numerically solving the equation

$$\ln(x) + \sum_{n=2}^{6}\frac{nB_n}{(n-1)v_{sat}^{n-1}}(x^{n-1} - 1) = -\frac{A_{ls}}{6\pi\rho_f k_B T}\frac{1}{\delta^3}. \tag{7}$$

Figure 3(a) shows the comparison of the present MD results with the classic theory based on Eq. (6) for the vapor pressure near a water thin film adsorbed on a gold substrate for the film thickness of 0.70 to 6.25 nm at 400 K. The MD results based on the Lennard-Jones and Spohr potentials for Au-H_2O interactions, as well as the 9-3 L-J mean field wall, are all included. The vapor pressure predicted by Eq. (6) shows good agreement with the MD results for a water film as thin as 0.70 nm, demonstrating that the classic disjoining pressure theory is adequate for predicting the disjoining pressure effect in a thin water film in the absence of surface charges (or the electrostatic interactions of Au-H_2O not considered).

As a liquid film adsorbs on a solid crystal, both in-plane and out-of-plane ordering relative to the surface normal can be observed.[22] Although Carey and Wemhoff[23] showed that the out-of-plane ordering of the liquid molecules does not affect the disjoining pressure, their model was unable to account for the in-plane ordering due to the lack of crystal structure of the mean field wall. In the present work, the effect of in-plane ordering on the disjoining pressure is investigated by comparing the vapor pressure near a thin film on a mean field wall against that on a real gold lattice. Figure 3(b) plots the scaled density profile (scaled with averaged density, ρ_0) of the water thin film along y, showing disordering for the case of a mean field wall as opposed to the crystal-like ordering of water film on a crystalline wall. The similarity of vapor pressures of the two cases, shown in Fig. 3(a), confirms that the in-plane ordering does not significantly affect the disjoining pressure. It is noted here that neither the out-of-plane nor the in-plane liquid ordering is considered in the classic disjoining pressure theory. The consistency between MD simulations and the theory prediction implies that near-wall liquid ordering does not play an important role in disjoining pressure.

Up to now, only van der Waals interactions between gold surface and water film are considered. Panella *et al.*[25] proposed that the classic theory cannot correctly predict the disjoining pressure when other interatomic interactions (e.g., electrostatic forces) become important. For water molecules near a gold wall, their averaged negative charge center deviates from the positive center and can hence induce net charges on the gold surface. Some gold atoms are able to coordinate as +1 and +3 and to deprotonate water. Because there is not a simple way to accurately calculate the induced charge density within classic MD simulations, we specify a range of charge density on the gold surface to examine its effect on disjoining pressure. The interactions between water and gold now involve two contributions: the van der Waals and electrostatic forces. While the Spohr potential is used to describe the van der Waals interactions between the water and gold, a cut-off Coulombic potential (cutoff distance of 9 Å) is used to describe the electrostatic interactions, with PPPM used to account for long-range Coulombic

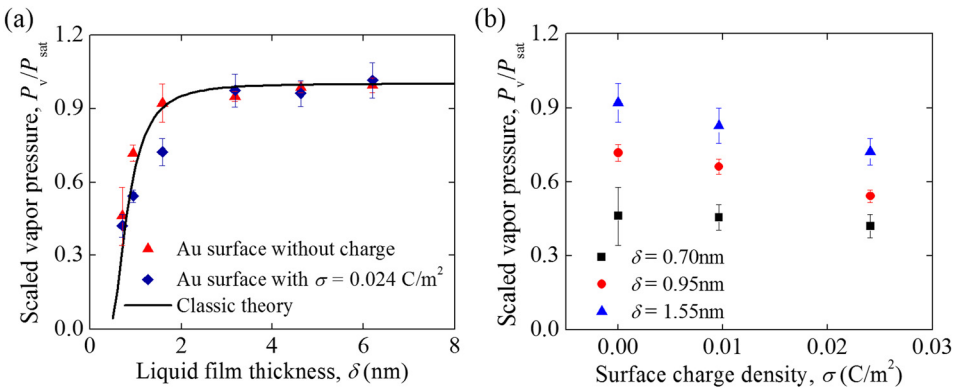

FIG. 4. Effect of electrostatic forces on vapor pressure near a water thin film adsorbed on a gold surface with different film thicknesses at 400 K. (a) Comparison of the vapor pressure on a gold surface with and without surface charges. (b) Vapor pressure as a function of surface charge density.

interactions. Figure 4(a) shows the vapor pressure near a water thin film adsorbed on a gold surface with and without surface changes for water film thickness values of 0.70–6.25 nm at 400 K. The charge density applied here is 0.024 C/m^2. A reduction in vapor pressure is observed for the film thickness smaller than 3 .15nm in the presence of electrostatic forces. For example, for a film thickness of $\delta = 0.95$ nm, P_v/P_{sat} decreases from 0.719 to 0.541 with $\sigma = 0.024$ C/m^2 and P_v/P_{sat} reduces from 0.921 to 0.723 for $\delta = 1.55$ nm. These results indicate the enhancement of the disjoining pressure effect due to surface charges. For $\delta > 3.15$ nm, the effect of surface charges on P_v/P_{sat} becomes too weak to be detected by present MD simulations. Figure 4(b) shows the vapor pressure of a water film for gold surface charge density range of 0 to 0.024 C/m^2 with film thicknesses of 0.70, 0.95, and 1.55 nm. For all three film thicknesses, the vapor pressure decreases (or the disjoining pressure increases) with the surface charge density. It is important to note that, the enhancement of the disjoining pressure effect due to electrostatic forces shown in Fig. 4 is consistent with experimental results of Panella *et al.*[25] for polar liquid thin films.

In summary, the disjoining pressure of an ultra-thin water film absorbed on a gold surface is investigated. The water vapor pressure is predicted using the classic disjoining pressure theory based on the 6th-order virial expansion for the water EOS and the Lennard-Jones potential for Au-H_2O interactions. The vapor pressure calculated by MD simulations in the absence of electrostatic interactions between gold and water, using the mean field wall, Lennard-Jones, and modified Spohr potentials for Au-H_2O interactions, respectively, agrees well with that predicted by the classic disjoining pressure theory. This result indicates that neither out-of-plane nor in-plane ordering of water films greatly affects the disjoining pressure. In the presence of electrostatic interactions between gold and water, the surface charges of the gold substrate are found to enhance the disjoining pressure of water thin film, consistent with that observed experimentally in polar liquid thin films.

Support for this work was provided by the National Science Foundation (No. DMR-1104835). Computational resources were provided by the Extreme Science and Engineering Discovery Environment (XSEDE) (Grant No. TG-CTS110056). Fruitful discussion with Professor Hai-Feng Ji in the Chemistry Department of Drexel University is greatly appreciated.

[1]C. M. Mate, J. Appl. Phys. **72**, 3084 (1992).
[2]H. B. Ma, G. P. Peterson, and D. M. Pratt, Microscale Thermophys. Eng. **2**, 283 (1998).
[3]K. Sefiane, Appl. Phys. Lett. **89**, 044106 (2006).
[4]D. Wasan, A. Nikolov, and K. Kondiparty, Curr. Opin. Colloid Interface Sci. **16**, 344 (2011).
[5]R. Xiao, S. C. Maroo, and E. N. Wang, Appl. Phys. Lett. **102**, 123103 (2013).
[6]J. J. Zhao, Y. Y. Duan, X. D. Wang, and B. X. Wang, Int. J. Heat Mass Transfer **54**, 1259 (2011).
[7]C. Li and G. P. Peterson, J. Heat Transfer **128**, 1320 (2006).
[8]H. B. Ma, P. Cheng, B. Borgmeyer, and Y. X. Wang, Microfluid. Nanofluid. **4**, 237 (2008).
[9]S. Narayanan, A. G. Fedorov, and Y. K. Joshi, Langmuir **27**, 10666 (2011).
[10]H. Wang, S. V. Garimella, and J. Y. Murthy, Int. J. Heat Mass Transfer **50**, 3933 (2007).
[11]Y. S. Ju, M. Kaviany, Y. Nam, S. Sharratt, G. S. Hwang, I. Catton, E. Fleming, and P. Dussinger, Int. J. Heat Mass Transfer **60**, 163 (2013).
[12]S. G. Kandlikar, Exp. Therm. Fluid Sci. **26**, 389 (2002).
[13]V. P. Carey, Exp. Heat Transfer **26**, 296 (2013).
[14]B. V. Derjaguin and N. V. Churaev, J. Colloid Interface Sci. **66**, 389 (1978).
[15]H. C. Hamaker, Physica **4**, 1058 (1937).
[16]I. E. Dzyaloshinskii, E. M. Lifshitz, and L. P. Pitaevskii, Adv. Phys. **10**, 165 (1961).
[17]B. Ninham, V. A. Parsegian, and G. Weiss, J. Stat. Phys. **2**, 323 (1970).
[18]J. N. Israelachvili and G. E. Adams, J. Chem. Soc., Faraday Trans. 1 **74**, 975 (1978).
[19]S. Biggs and P. Mulvaney, J. Chem. Phys. **100**, 8501 (1994).
[20]B. Y. Derjaguin, V. M. Muller, and Y. Rabinovich, Kolloidn. Zh. **31**, 304 (1969).
[21]R. G. Horn, D. R. Clarke, and M. T. Clarkson, J. Mater. Res. **3**, 413 (1988).
[22]J. N. Israelachvili, *Intermolecular and Surface Forces: Third Revised Edition* (Elsevier Science, San Diego, 2011).
[23]V. P. Carey and A. P. Wemhoff, ASME Trans. J. Heat Transfer **128**, 1276 (2006).
[24]E. S. Sabisky and C. H. Anderson, Phys. Rev. A **7**, 790 (1973).
[25]V. Panella, R. Chiarello, and J. Krim, Phys. Rev. Lett. **76**, 3606 (1996).
[26]B. V. Derjaguin and N. V. Churaev, J. Colloid Interface Sci. **49**, 249 (1974).
[27]D. Bhatt, J. Newman, and C. J. Radke, J. Phys. Chem. B **106**, 6529 (2002).
[28]M. Han, J. Mech. Sci. Technol. **26**, 2275 (2012).
[29]S. C. Maroo and J. N. Chung, J. Appl. Phys. **106**, 064911 (2009).
[30]J. Yu and H. Wang, Int. J Heat Mass Tranfer **55**, 1218 (2012).
[31]H. Reza Seyf and Y. Zhang, J. Heat Transfer **135**, 121503 (2013).
[32]S. C. Maroo and J. N. Chung, J. Heat Transfer **135**, 041501 (2013).
[33]M. Han, Colloids Surf., A **317**, 679 (2008).
[34]M. S. Daw, S. M. Foiles, and M. I. Baskes, Mater. Sci. Rep. **9**, 251 (1993).
[35]H. W. Horn, W. C. Swope, J. W. Pitera, J. D. Madura, T. J. Dick, G. L. Hura, and T. Head-Gordon, J. Chem. Phys. **120**, 9665 (2004).
[36]J. P. Ryckaert, G. Ciccotti, and H. J. C. Berendsen, J. Comput. Phys. **23**, 327 (1977).

[37]K. Tay and F. Bresme, J. Mater. Chem. **16**, 1956 (2006).
[38]S. Plimpton, J. Comput. Phys. **117**, 1 (1995).
[39]See supplementary material at http://dx.doi.org/10.1063/1.4858469 for the method of calculating the interaction energy per unit area between two gold substrates across a thin water film.
[40]V. A. Parsegian and G. H. Weiss, J. Colloid Interface Sci. **81**, 285 (1981).
[41]A. Harasima, in *Advances in Chemical Physics* (John Wiley & Sons, Inc., New York, 2007), p. 203.
[42]Y. S. Dou, L. V. Zhigilei, N. Winograd, and B. J. Garrison, J. Phys. Chem. A **105**, 2748 (2001).
[43]K. M. Benjamin, J. K. Singh, A. J. Schultz, and D. A. Kofke, J. Phys. Chem. B **111**, 11463 (2007).